

Spring Arctic Oscillation-East Asian summer monsoon connection through circulation changes over the western North Pacific

Dao-Yi Gong · Jing Yang · Seong-Joong Kim ·
Yongqi Gao · Dong Guo · Tianjun Zhou ·
Miao Hu

Received: 9 May 2010 / Accepted: 1 March 2011 / Published online: 12 March 2011
© Springer-Verlag 2011

Abstract In the present study the links between spring Arctic Oscillation (AO) and East Asian summer monsoon (EASM) was investigated with focus on the importance of the North Pacific atmospheric circulation and sea surface temperature (SST). To reduce the statistical uncertainty, we analyzed high-pass filtered data with the inter-annual time scales, and excluded the El Niño/Southern Oscillation signals in the climate fields using a linear fitting method. The significant relationship between spring AO and EASM are supported by the changes of multi-monsoon components, including monsoon indices, precipitation, and three-dimensional atmospheric circulations. Following a stronger positive spring AO, an anomalous cyclonic circulation at 850 hPa appears in southeastern Asia and the western North Pacific in summer, with the easterly anomalies spanning from the Pacific to Asian continent along 25°N–30°N and the westerly anomalies south of 15°N. At the same time, the

summer western North Pacific subtropical high becomes weaker. Consistently, the positive precipitation anomalies are developed over a broad region south of 30°N stretching from southern China to the western Pacific and the negative precipitation anomalies appear in the lower valley of the Yangtze River and southern Japan. The anomalous cyclone in the western North Pacific persisting from spring to summer plays a key role in modulating EASM and monsoon precipitation by a positive air-sea feedback mechanism. During spring the AO-associated atmospheric circulation change produces warmer SSTs between 150°E–180° near the equator. The anomalous sensible and latent heating, in turn, intensifies the cyclone through a Gill-type response of the atmosphere. Through this positive feedback, the tropical atmosphere and SST patterns sustain their strength from spring to summer, that consequently modifies the monsoon trough and the western North Pacific subtropical high and eventually the EASM precipitation. Moreover, the SST response to AO-circulation is supported by the numerical simulations of an ocean model, and the anomalous atmospheric circulation over the western North Pacific is also reproduced by the dedicated numerical simulations using the coupled atmosphere–ocean model. The observation evidence and numerical simulations suggest the spring AO can impact the EASM via triggering tropical air-sea feedback over the western North Pacific.

D.-Y. Gong (✉) · J. Yang · D. Guo · M. Hu
State Key Laboratory of Earth Surface Processes and Resource Ecology, Beijing Normal University, 100875 Beijing, China
e-mail: gdy@bnu.edu.cn

S.-J. Kim
Korea Polar Research Institute, Incheon, Korea

Y. Gao · D. Guo
Nansen-Zhu International Research Center,
IAP/CAS, 100029 Beijing, China

Y. Gao
Nansen Environmental and Remote Sensing Center/Bjerknes
Center for Climate Research, Bergen, Norway

T. Zhou
State Key Laboratory of Numerical Modeling for Atmospheric Sciences and Geophysical Fluid Dynamics (LASG), IAP/CAS, 100029 Beijing, China

Keywords Arctic Oscillation · East Asian summer monsoon · North Pacific · Air-sea interaction

1 Introduction

To skillfully predict the East Asian summer monsoon (EASM) is a challenging issue for climate community,

which relies heavily on our better understanding of EASM variability. Previous analyses have noted an evident linkage between winter-spring Arctic Oscillation (AO)/North Atlantic Oscillation (NAO) and the EASM. By analyzing observed precipitation during the 20th century, Gong and Ho (2003) found a significant out-of-phase correlation between the late spring AO index and boreal summer rainfall along the Meiyu-Changma-Baiu rain-belt on interannual time scales. The Asian climate-AO/NAO links are also evident at the interdecadal timescales as revealed by long historical climate records and proxies (Fu and Zeng, 2005; Feng and Hu 2008). Their time-lag relationship serves well as summer monsoon predictors. For example, Wu et al. (2009a) used spring NAO and El Niño/Southern Oscillation (ENSO) indices as precursory indicators to forecast the EASM, and found that the statistical model taking into account only these two factors shows predictive skill comparable to 14 state-of-the-art climate model ensembles.

The responsible mechanism(s) how winter/spring AO influence summer climates over East Asia and how AO's memories persist for a couple of months, however, are not well understood. Some explanations were suggested by previous studies where the importance of land or ocean thermal anomalies was highlighted. By producing anomalous temperatures over the Eurasian continent in winter and spring, AO could keep its influence on Asian climates until the following summer (Chang et al. 2001; Buermann et al. 2005; Goswami et al. 2006; Feng and Hu 2008). For example, Chang et al. (2001) reported that in association with positive NAO and strengthened/poleward shift of the jet stream over the North Atlantic in winter, the temperature anomalies in western Europe could extend eastward to most of northern Eurasia until spring. This might result in an anomalous thermal contrast between the Eurasian continent and neighboring lands/oceans, disturbing the monsoon activity. Buermann et al. (2005) obtained a similar result that the AO-induced winter/spring temperature anomalies could push the mid-Eastern jet poleward during negative AO phases, resulting in an anomalous surface heating and drying that persist until the later spring and finally affect the Indian monsoon rainfall in June. The continental snow related to AO (Bamzai 2003; Hori and Yasunari 2003) has multi-month memories in influencing regional temperature/moisture and may also act as an anomalous heating forcing of summer climate over East Asia (Ogi et al. 2004; Wu et al. 2009b). Some recent observation and simulation studies emphasized the importance of the North Atlantic sea surface temperature (SST) in maintaining the AO's memories on interannual time scales as well as on the decadal time scales, where the SST-forced atmospheric fluctuations result in Asian summer monsoon responses through westerly wind, jet stream, and

wave activities (Goswami et al. 2006; Lu et al. 2006; Sung et al. 2006; Feng and Hu 2008; Wang et al. 2009; Wu et al. 2009a). Ogi et al. (2004) reported that the winter NAO persistently influences the sea ice and SSTs in the Arctic from winter to summer, and warm signals around the Barents Sea region excite the Rossby waves propagating toward the Sea of Okhotsk, thus a positive phase of January NAO being accompanied by a stronger Okhotsk High in June. Yu and Zhou (2004) and Li et al. (2005) reported the upper troposphere cooling in association with positive-phase NAO, which spread from northern Africa/Southern Europe in winter/spring to East Asia in June–September. This might result in southward shift of the jet stream, and a corresponding weaker summer monsoon. Note that these studies concerning spring AO/NAO-EASM put much attention on the persistent anomalies of boundaries or/and atmospheric circulation over upstream regions (i.e., Eurasian continent and North Atlantic). With regard to their teleconnections to Asian climate, the quasi-stationary Rossby waves are often suggested to propagate these AO-related anomalies eastward to East Asia (Branstator 2002; Watanabe 2004). In addition, the summer AO/NAO also exerts climate influence over North Hemisphere (Folland et al. 2009). The dynamics of AO itself might be involved in the multi-month connection, even though the observed AO persistence from spring to summer is somewhat weak. The EASM is strongly influenced by atmospheric and oceanic states over the North Pacific and the influence of ENSO on East Asian climates has attracted much attention. Note that observed evidence suggests that the air-sea conditions over western Pacific might also be directly or indirectly modulated by AO (Miller et al. 2003; Thompson and Lorenz 2004; Nakamura et al. 2006; Gong et al. 2009). The possible roles of the North Pacific atmospheric circulation and SSTs in linking spring AO and EASM, however, have not been clearly addressed by previous studies.

The main goal of the present study is to explore the atmospheric circulation and SST changes in the North Pacific in association with spring AO, and further to investigate the possible roles of the North Pacific in maintaining the spring AO-EASM connection. The rest of the paper is organized as follows. Section 2 describes the data and methods used in the study. Section 3 first presents the statistical relationship between spring AO and summer monsoon indices, and then briefly demonstrates the summer anomalies of precipitation and regional circulations in association with spring AO. In Sect. 4 the possible mechanisms connecting spring AO and EASM are investigated by time-lag analysis of atmospheric circulation, SSTs, and diabatic heating variations over the North Pacific, which are followed by a hypothetical explanation of the mechanism. The reproducibility of AO-forced SST anomalies and the summer atmospheric circulation changes are

investigated by numerical simulations and presented in Sect. 5. The temporal stability of spring AO-EASM relationship has been discussed in Sect. 6. Finally, the major finding of the study is given in Sect. 7.

2 Data and method

Atmospheric circulation data used in the study are taken from the National Centers for Environmental Prediction–National Center for Atmospheric Research (NCEP–NCAR) reanalysis (Kalnay et al. 1996) data, including daily and monthly geopotential heights at 500 hPa and winds at 850 and 200 hPa with a horizontal resolution of 2.5° latitude \times 2.5° longitude. The AO index is the corresponding time coefficients of the first empirical orthogonal function (EOF) of the monthly sea level pressures (SLP) north of 20°N (Thompson and Wallace 1998). The spring AO index is the average for March, April and May. In addition, the gridded monthly extended reconstructed sea surface temperature (ERSST v3b) with a resolution of 2° latitude \times 2° longitude (Smith et al. 2008) and the GPCP combined precipitation (v2.1) (Adler et al. 2003) with a resolution of 2.5° latitude \times 2.5° longitude are used. All analysis are confined within a common data period of 1951–2008, except for GPCP precipitation of which the analysis period is 1979–2008. Wang et al. (2008a) pointed out that the seasonally evolving spatial pattern of the EASM remains relatively unchanged during whole summer monsoon season, and persists through the May–August season (Wang et al. 2008a, figure 6a). Therefore, when dealing with summer monsoon climate we used the mean for June–August. Of all climate variables analyzed in the present study, we focus only on their interannual variations. Thus, prior to analysis all climate time series are high-pass filtered by using a Butterworth filter, and only the components with time periods shorter than 10 years are remained and employed in the following analysis.

Climates over the northwestern Pacific and East Asia are largely impacted by ENSO (e.g., Wang 2000, among many others). We removed ENSO signals in the variables of interest by means of regression analysis. Since ENSO has a phase-locking feature with a mature peak in boreal winter, we simply fit the Niño3 SST from boreal winter-spring (i.e. from the preceding December to May) to climate variables by using the least-square technique. Then the estimated ENSO-related components are subtracted from climate time series, the residuals are regarded as ‘ENSO-free’ parts and subjected to the analysis. We also tested Niño3.4 SST for comparison, and obtained almost the same results, implying that the corresponding changes in atmosphere are not sensitive to the choice of Niño SSTs.

3 EASM-AO links

3.1 Correlations between spring AO and EASM indices

First, we analyzed the statistical relationship between March–April–May (MAM) AO and June–July–August (JJA) monsoon. Three EASM indices are investigated, including Wang and Fan (1999) index, Zhang et al. (2003) index, and Lau et al. (2000) index. Their definitions are as follows.

Wang and Fan (1999) index: $U_{850}(5^\circ\text{N}–15^\circ\text{N}, 90^\circ\text{E}–130^\circ\text{E})$ minus $U_{850}(22.5^\circ\text{N}–32.5^\circ\text{N}, 110^\circ\text{E}–140^\circ\text{E})$;
Zhang et al. (2003) index: $U_{850}(10^\circ\text{N}–20^\circ\text{N}, 100^\circ\text{E}–150^\circ\text{E})$ minus $U_{850}(25^\circ\text{N}–35^\circ\text{N}, 100^\circ\text{E}–150^\circ\text{E})$; and
Lau et al. (2000) index: $U_{200}(40^\circ\text{N}–50^\circ\text{N}, 110^\circ\text{E}–150^\circ\text{E})$ minus $U_{200}(25^\circ\text{N}–35^\circ\text{N}, 110^\circ\text{E}–150^\circ\text{E})$,

Here U_{850} and U_{200} denote the mean zonal wind at 850 hPa and 200 hPa levels, respectively. The difference of U_{850} between the two areas measures the horizontal wind shear, reflecting the vorticity variations in lower troposphere, while the U_{200} difference reflects dynamical aspects of upper circulations. Among about two dozens of EASM indices often employed in monsoon climate studies, the definition by Wang and Fan (1999) has the highest skill in capturing the total variance of precipitation and three-dimensional circulation over East Asia (Wang et al. 2008a). Figure 1a displays the time series of MAM AO and JJA monsoon indices. Their interannual variations have an in-phase relationship in general, and the larger (smaller) JJA monsoon indices tend to accompany the higher (lower) MAM AO conditions. For the whole time period from 1951 to 2008, the Wang and Fan (1999) EASM index and the spring AO yield a significant (at the 95% level) Pearson’s correlation of $+0.33$. This implies that following high MAM AO the horizontal wind shear at 850 hPa level over East Asia tends to be enhanced in JJA. This features a significantly positive EASM index. Does this MAM AO related horizontal circulation anomalies appear only in lower troposphere (say 850 hPa)? To answer this question we investigated the zonal wind (u), meridional wind (v), and vertical wind (w) for the whole troposphere. Figure 1b demonstrates the wind anomalies in a pressure-latitude section along 120°E . An anomalous easterly wind (>0.5 m/s) center is located in approximately 30°N and stretches vertically from 1,000 to 200 hPa. Meanwhile, the westerly anomalies appear in south of 20°N below about 400 hPa. These features clearly confirm that following positive MAM AO, anomalous westerlies exist from surface to mid-troposphere in tropics and anomalous easterlies appear from surface to about 200 hPa at 30°N in JJA. Thus we would conclude that the AO-related circulation anomalies

in summer are not confined to the lower troposphere, but are manifested in the whole troposphere with well-defined vertical structures.

Note that the zonal wind anomalies near surface are located slightly north of the latitudes defined by Wang and Fan (1999) monsoon index. Taking this feature into account, we re-computed the monsoon-AO correlation using Zhang et al. (2003) monsoon index, and reasonably yielded a slightly larger correlation coefficient of +0.35. In addition, the upper tropospheric circulation is one of the important aspects of EASM. The anomalous easterlies around 30°N and westerlies around 45°N (Fig. 1b) resembles quite well the EASM-related 200 hPa zonal wind changes such as the regional monsoon circulation pattern of Lau et al. (2000), and the AO-related upper circulation anomalies also resemble the zonal wind pattern related to the monsoon precipitation (Gong and Ho 2003), consistent with the anomalous vertical air motion related to the westerly jet stream.

The quality of reanalysis datasets and precipitation data was improved after the late 1970s with the usage of satellite observation. To confirm the robustness of AO-monsoon correlations, we re-computed the relations between spring AO and three summer monsoon indices for a shorter data period of 1979–2008. As shown in Table 1, the MAM AO is significantly correlated with all three EASM indices. The correlation coefficients are $r = +0.47$ for Wang and Fan (1999) index, $r = +0.44$

for Zhang et al. (2003) index, and $r = +0.40$ for Lau et al. (2000) index, respectively. These similar correlations are all significant at the 95% level. Again, the consistent and significant correlations between AO and three monsoon indices confirm the significance of the EASM-spring AO connection. These statistical analyses show that the MAM AO accounts for about 19% variance of the total inter-annual variability of monsoon indices. Comparing to the ENSO-explained variance (41%), the amount related to the AO is a large portion. These values are similar to the results of Wu et al. (2009a) even though they used slightly different NAO and ENSO indices. It is clear that MAM AO is an important contributor to the inter-annual variability of the EASM.

3.2 Summer precipitation anomalies

Precipitation is one of the dominant aspects of the EASM. Previous analysis of summer precipitation revealed that the leading mode of rainfall over East Asia has a south–north dipole structure which is coherently related to the three-dimensional monsoon circulation variability. Taking both precipitation and large-scale circulation into account, Wang et al. (2008a) carried out a multi-variable EOF analysis, and found that the precipitation component of the major spatial mode had a north–south dipole pattern with two opposite anomalous regions. One is located over the northern South China Sea and the Philippine Sea with a

Fig. 1 **a** Time series of March–April–May AO and June–July–August monsoon indices of Wang and Fang (1999) and Zhang et al. (2003). **b** Pressure–latitude section along 120°E showing the JJA anomalies of zonal (u), meridional (v) and vertical (w) winds in association with a one-unit-larger MAM AO index. To facilitate comparison, w has been multiplied by 1,000. The w , v are shown as vectors and u as contours with intervals of 0.4 m s^{-1} . Shadings indicate significant u at the 95% level

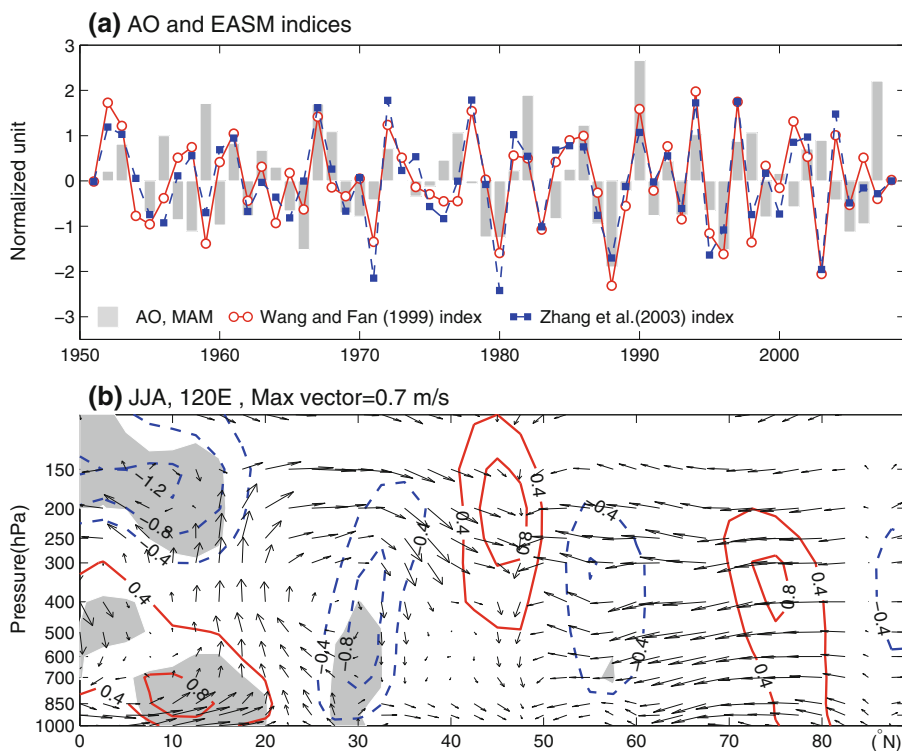


Table 1 Correlation coefficients among MAM AO and JJA monsoon indices and regional precipitation for the period 1979–2008

	Wang and Fan (1999) index, JJA	Zhang et al. (2003) index, JJA	Lau et al. (2000) index, JJA	South Precip, JJA	North Precip, JJA
AO, MAM	+0.47 ^a	+0.44 ^a	+0.40 ^a	+0.37 ^a	−0.22
South Precip ^c , JJA	+0.69 ^b	+0.65 ^b	+0.72 ^b	–	−0.46 ^a
North Precip ^d , JJA	−0.48 ^b	−0.56 ^b	−0.64 ^b	−0.46 ^a	–

^a Significant at the 95% level

^b Significant at the 99% level

^c Mean precipitation averaged over the southern region over 15°N–30°N, 110°E–135°E

^d Mean precipitation averaged over the northern region over 30°N–35°N, 110°E–135°E

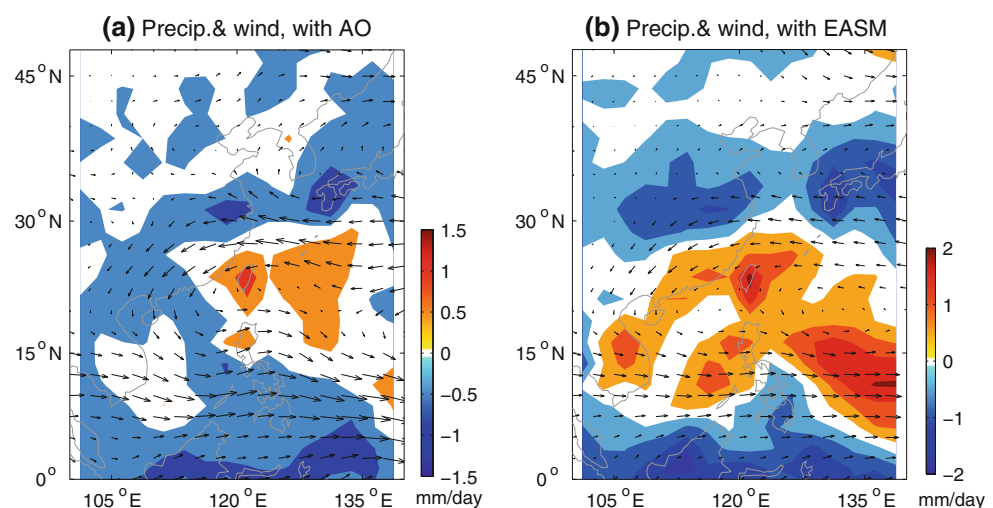
west-east orientation, and the other spans from the Yangtze River valley to southern Japan, which covers the prevailing Meiyu-Changma-Baiu frontal area. In the previous section, we demonstrate the significant association between summer monsoon indices and spring AO. Their physical concordance would be supported by year-to-year fluctuations of monsoonal precipitation and by the regional contrast between these two dipole regions of the leading mode.

To confirm this feature, here, we investigated the JJA precipitation in association with MAM AO. After excluding ENSO signals, we computed the regression coefficients of summer precipitation upon the spring AO. The distribution of the JJA precipitation anomalies (i.e., the regression coefficients) corresponding to a one-standard-deviation positive MAM AO index were plotted based on data from 1979 to 2008 in Fig. 2. A dipole pattern in the East Asia clearly appears as the outstanding feature. Positive anomalies are found over a broad region south of approximately 30°N, spanning from southern China to western Pacific. The large anomalies of >0.5 mm/day are located in around (15°N–30°N, 110°E–135°E) with centers (>1 mm/day) in Taiwan and in east of Okinawa. Meanwhile, to the north of 30°N there are negative precipitation anomalies appearing in the lower valley of Yangtze River and southern Japan.

Since these regression coefficients are estimated only based on the linear components statistically relating to AO, the spatial pattern corresponding to negative AO is certainly the same but all anomalies are of opposite signs. For comparison we also plotted the JJA precipitation in association with summer monsoon index of Wang and Fan (1999) and displayed together. The major spatial pattern of AO-related precipitation anomalies surprisingly resembles the monsoon-related pattern with above-normal precipitation in south of about 30°N and below-normal precipitation to the north. The similarity of spatial structure again suggests the close connection of EASM rainfall to the preceding spring AO.

We also analyzed the detailed temporal variations of precipitation and their consistency with monsoon/AO focusing on the two centers of the anomalies as revealed in above analysis. For the south center, a regional mean time series is obtained by averaging JJA rainfall from 15°N–30°N and 110°E–135°E. The GPCP summer precipitation for this region is significantly correlated with MAM AO index at +0.37 for period 1979–2008. Not surprisingly, the interannual variations of precipitation are also highly connected to monsoon indices. Table 1 lists correlations between south precipitation with monsoon indices,

Fig. 2 Spatial distribution of the regression coefficients of precipitation and 850 hPa wind in JJA upon the spring AO (a) and upon June–July–August Wang and Fan (1999) index (b). Colors are precipitation in mm per day. Vectors are 850 hPa winds (m s^{-1}), and the maxima in (a) and (b) are 1.2 and 2.4 m s^{-1} , respectively. Data periods are 1979–2008. All regression coefficients are results after removing ENSO signals. Values in (a) and (b) are scaled to correspond to one standard deviation of AO and EASM indices, respectively



$r = +0.69$ for Wang and Fan (1999) index, $r = +0.65$ for Zhang et al. (2003) index, and $r = +0.72$ for Lau et al. (2000) index. This indicates that more summer precipitation would occur in this region in high EASM summers, which is more likely to be accompanied by the high-AO in springs. For the north center where negative precipitation anomalies appear, we simply chose a neighboring region of 30°N – 35°N , 110°E – 135°E to make the regional mean. Summer precipitation in the two regions has an evident out-of-phase relationship, correlation between them is -0.46 . On the inter-annual time scales, its correlation with three monsoon indices varies from -0.48 to -0.64 , all significant. However, it is correlated with the spring AO at only a moderate level, $r = -0.22$, not significant.

The boreal summer Meiyu-Changma-Baiu precipitation along Yangtze River to southern Japan is an important indicator of EASM variability. The coarser grid GPCP precipitation along this belt has only a moderate correlation with MAM AO. Note that Gong and Ho (2003) reported a significant relation between late spring AO and precipitation along the rain-belt by analyzing surface observation data for 10 stations along the rain-belt, including Shanghai, Nanjing, Jiujiang, Wuhan, Guiyang, Changsha, Tokyo, Osaka, Kagoshima, and Izuhara. Among all seasons the mean summer rainfall has a maximum correlation with May AO on the inter-annual time scales ($r = -0.45$, for 1900–1998 data period). For clarity, here we re-calculated their correlations using the mean precipitation time series (Gong and Ho 2003, figure 2). When the ENSO signals excluded, the mean summer precipitation averaging from 10 stations correlates with MAM AO at a value of -0.34 , significant at the 95% level. Its correlations with three monsoon indices are respectively -0.42 for Wang and Fan (1999) index, -0.42 for Zhang et al. (2003) index, and -0.59 for Lau et al. (2000) index. This suggests that the spring AO signals could be well reflected in longer station precipitations in the Meiyu-Changma-Baiu belt. Somewhat weaker relations in GPCP data might be due to the coarser spatial resolution and shorter data period. The consistent and significant correlations among EASM indices, regional precipitation, and AO index support the robustness of spring AO-summer monsoon climate connections (Table 1).

3.3 Regional anomalies of 850 hPa winds and 500 hPa heights

The western North Pacific monsoon trough and subtropical high (WNPSH) are two important subsystems of the EASM circulation system (Tao and Chen 1987). How do AO-related summer precipitation anomalies and AO-monsoon index correlations as discussed above coincide

with the corresponding variations of the trough and WNPSH? The low-level trough is the major system that produces most of the summer monsoon rainfall. Firstly, we analyzed the atmospheric circulation anomalies at 850 hPa level to investigate the possible changes of the trough. The regression coefficients of the horizontal winds upon the MAM AO for 1979–2008 are shown in Fig. 2. The most outstanding feature of AO-related wind changes is an anomalous cyclonic circulation in the southeastern Asia and western Pacific. The strengthened easterly anomalies span from Pacific to continent along 25°N – 30°N , which become the anomalous north winds in 105°E – 110°E , and then flow eastward south of 15°N . We also computed the regression coefficients of 850 hPa winds upon the monsoon index of Wang and Fan (1999). The corresponding spatial pattern is almost identical to that for AO-related anomalies. This kind of cyclonic pattern has been revealed to be the inherent mode of EASM in previous studies (e.g. Wang and Fan, 1999; Wang et al. 2008a, b; among many others). Comparing with Fig. 1, we can find that in association with positive MAM AO, there is an anomalous upward air motion in 15°N – 25°N along 120°E , which corresponds to the location of the cyclone. The tropospheric downward air motion appearing in about 30°N – 35°N (Fig. 1b) is also consistently accompanied by the anti-cyclonic horizontal shear which is located to the north of 30°N over East Asia (Fig. 2a). In addition, as demonstrated in Fig. 1b, the zonal winds in tropics have a significant difference between the lower and the upper troposphere. In south of 20°N , the anomalous easterly winds (-0.4 to -1.2 m/s) appear from 300 to 100 hPa, meanwhile the anomalous westerly winds ($+0.4$ to $+0.8$ m/s) exist below 400 hPa. This feature implies an enhanced vertical wind shear, being a favorable condition for trough activity in lower levels. These features of trough anomalies clearly imply that following an above-normal spring AO, the lower-level trough would be intensified in the south-southeast Asia, at the same time tends to weaken along the Meiyu-Changma-Baiu rain belt. These would consistently explain why there is the tendency of more JJA precipitation in south of 30°N , and less JJA precipitation between 30°N – 35°N in high MAM AO years.

We further examined the changes of the WNPSH. In the middle troposphere, the WNPSH plays an important role in modulating moisture transporting and the rain-belt locations. Summer Meiyu-Changma-Baiu rainfall is significantly connected to the WNPSH on both inter-annual and decadal time scales. When the WNPSH intensifies or moves southward or extends westward, above-normal precipitation is expected to occur along the Yangtze River to southern Japan. When the WNPSH shifts northward to the normal latitude or retreats eastward, a drier condition

tends to take place there (Chang et al. 2000a, b; Gong and Ho 2002). To explore the possible changes of WNPSH, the 500 hPa height correlations with AO are analyzed and displayed (Fig. 3). In positive MAM AO years, the 500 hPa heights in summer are significantly lower than normal in the western Pacific, suggesting a weaker subtropical high or an eastward retreat. The 500 hPa heights in western flank of the climatological location of WNPSH can capture the variations of the WNPSH. The western Pacific near Taiwan has the largest standard deviation of inter-annual variability (Sui et al. 2007). To measure the WNPSH variability, we simply make a time series of the regional mean 500 hPa heights averaging from 120°E–135°E and 15°N–25°N where significant correlations are located. This region is close to the domain used in Gong and Ho (2002) and Sui et al. (2007). The MAM AO and JJA WNPSH indices evidently co-vary in an out-of-phase relation. For the period of 1951–2008, the WNPSH correlates with MAM AO at $r = -0.33$. Their out-of-phase relationship is more prominent from the late 1970s (Fig. 3b). In the period 1979–2008, two time series correlate at -0.48 , a much stronger connection. The WNPSH is known to be strongly modulated by ENSO SSTs. It is interesting to note that the WNPSH extremes show no covariations with strong ENSO events such as 1997/1998, 1981/1982, 1986/1987, and so on. This implies that the method of removing ENSO influence on circulation, SST and precipitation applied in the present study likely works well, and the statistical relationship between AO and EASM climates is very likely independent of ENSO. The weakened WNPSH would consequently reduce the meridional moisture transport and facilitate the low-level trough activity, being a condition favorable for precipitation in the southern East Asia.

4 Possible mechanisms for the linkage

4.1 Basin scale circulation anomalies in the North Pacific from MAM to JJA

An arisen question is how the JJA atmospheric anomalies over East Asia have established following a positive MAM AO. To shed light on this problem, we investigated the atmospheric circulation and SST anomalies over the whole North Pacific with analysis seasons extending from JJA back to MAM. The results are shown in Figs. 4 and 5. Generally, in association with AO, there are well-organized patterns in the North Pacific. The anomalies in 850 hPa winds and 500 hPa heights revealed in the previous sections are not regional phenomena confined to East Asia, but they are parts of the basin-scale anomalous structures. Surprisingly, the dominant features (particularly the anomalies in southeastern Asia and the western tropical Pacific) persist from MAM to JJA. During spring, the anomalous cyclone over the tropical North Pacific is prominent between 120°E–160°W at 850 hPa and an anomalous anticyclone is located over the extratropics. The similar large-scale patterns are also found in 500 hPa heights (Fig. 5) and 200 hPa streamlines, suggesting a barotropic structure in month-seasonal mean circulations. This kind of AO-related circulation pattern has also been documented by other studies. For example, Nakamura et al. (2007, figure 1b) obtained a similar cyclonic circulation pattern in boreal spring over the tropical North Pacific using a shorter Reanalysis II data (1979–2004). Associated with the atmospheric circulation, there are well-defined patterns in SST anomalies, too. In spring, there are positive SST anomalies in central to eastern Pacific south of 15°N, and at the same time significant cooling SSTs are located to

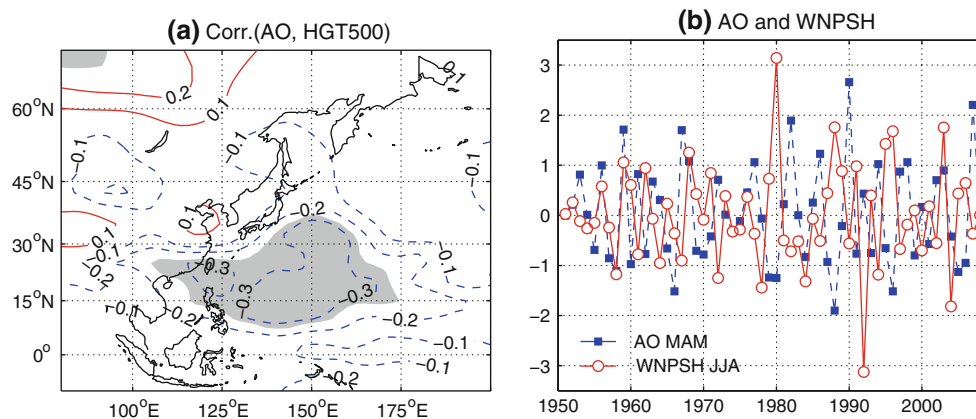


Fig. 3 **a** Correlations of June–July–August 500 hPa geopotential heights with March–April–May AO index, and the *shadings* indicate *grids* significant at the 95% level. **b** Comparison of spring AO time series with the summer western North Pacific Subtropical high

(WNPSH), which is defined as the regional mean 500 hPa heights averaging from 15°N–25°N and 120°E–135°E. Both normalized to facilitate comparison

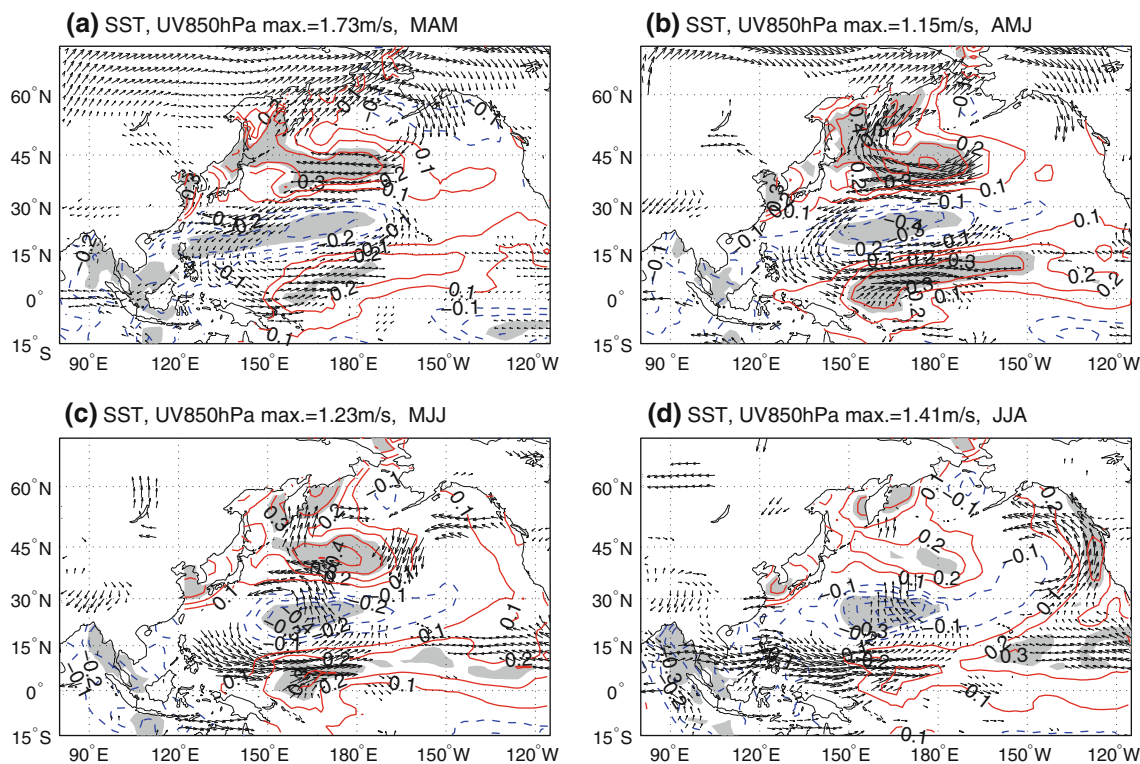


Fig. 4 Contour lines are correlation coefficients between AO and SST (solid lines: positive correlations, and dashed the negative, shadings: significant at the 95% level). The vectors are significant (95% level) anomalies of 850 hPa wind corresponding to one-unit-

larger MAM AO index. In all figures, AO index is confined to MAM while SSTs and winds are gradually changing from MAM to JJA. All shown are for interannual time scale and ENSO signals were removed

the north, centering in around 150°E – 180° , 15°N – 30°N . Yang et al. (2002) divided the winter SST variability in the North Pacific into ENSO-related and non-ENSO components, which account for 34.4% and 17.0% of the total variance, respectively. It is interesting to note that the non-ENSO components shows a dipole pattern with reverse SST anomalies between the extratropical North Pacific and the tropics, and is tightly linked to the westerly jet stream. These features suggest that the AO or westerly-related atmosphere circulations play essential roles in producing the SST anomalies. The cyclonic circulation would be responsible for the cooling in central Pacific with center located in 15°N – 30°N , 140°E – 180° by upwelling induced by the enhanced Ekman pumping as well as by evaporation due to the larger winds.

It is important to indicate that from MAM to JJA the tropical cyclonic anomalies at 850 hPa wind field and 500 hPa heights are similar in location and strength, while the western flank of the anomaly cyclone clearly extends westward from about 120°E in MAM to 105°E in JJA. The same is true for the underlying SST pattern, being persistently cool in the central Pacific and warmer in the central tropics. In contrast to tropical circulation and SST, the significant anomalies in the extratropical anticyclone and SSTs weaken quickly after MAM, and almost

disappear in JJA. Note that the AO becomes most active during the boreal winter. Are the MAM SSTs linked to the AO signals prior to spring? To clarify this we investigated the correlations between winter SSTs and MAM AO index, and found that there are no large-scale SST patterns during DJF. The significant negative correlations appear only in a small region to the east of Taiwan. No evident SST anomalies were found in tropics south of 15°N . We also examined the SSTs and circulations in association with DJF AO. Warmer SSTs appear in 30° – 40°N in DJF, and weaken in MAM. Over the tropics, negative SSTs are located in west of 170°E (figures not shown). These SST features are remarkably different from those in MAM through JJA. The anomalous SSTs in MAM and JJA would be viewed as a response to AO rather than a forcing to AO, which is confirmed by the numerical simulations and discussed in Sect. 5. The substantial and persistent anomalies of the atmospheric circulation and SSTs over tropics provide clues to the possible mechanism responsible for the ‘long-memory’ of AO-SST-monsoon connection which keeps climate anomalies from spring to summer. The maintenance of the tropical cyclone and warming SST is suggested to be due to the air-sea interaction as discussed later.

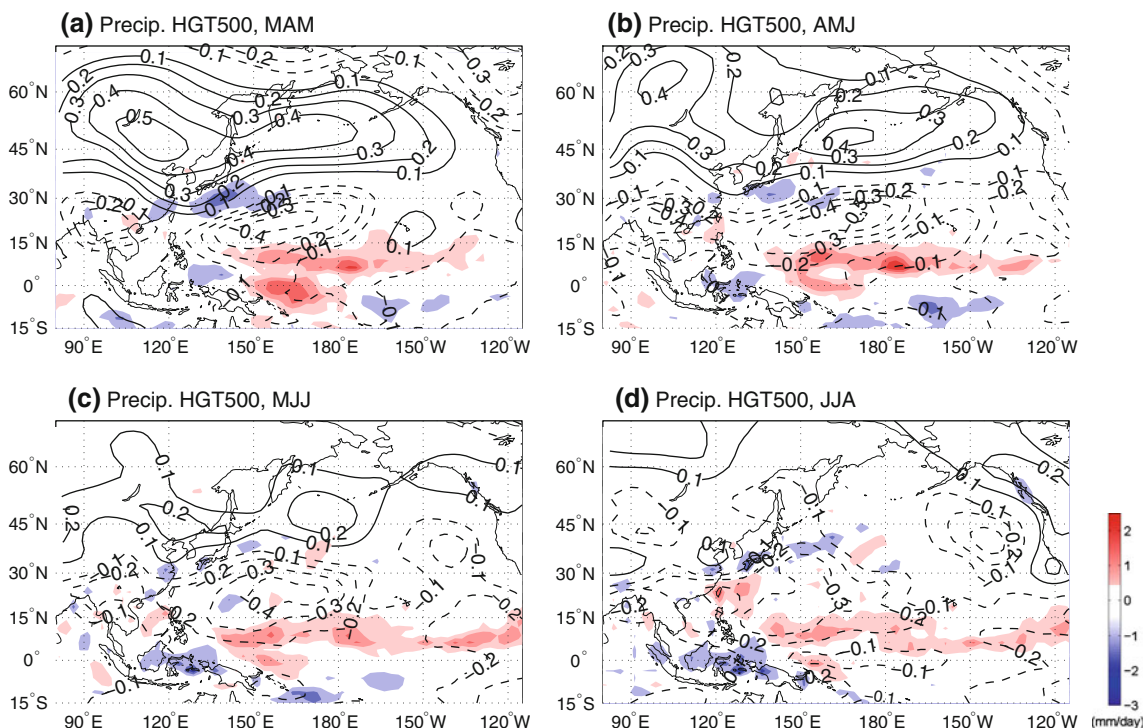


Fig. 5 Contour lines are correlation coefficients between AO and geopotential height at 500 hPa (solid lines: positive correlations, and dashed the negative). The color shadings are precipitation anomalies (GPCP data period: 1979–2008) corresponding to one-unit-larger AO

index. In all figures, AO index is confined to MAM while 500 hPa heights and precipitation are gradually changing from MAM to JJA. All shown are for interannual time scale and ENSO signals have been removed

4.2 Anomalous heating in association with MAM AO

As shown above, accompanying with the AO-related circulation, there are large-scale SST anomalies. The roles of tropical Pacific SSTs in influencing EASM have been emphasized by numerous observational and numerical studies. Besides the Niño SSTs, the western Pacific and Indian Ocean SSTs also exert evident influence through modulating regional atmospheric circulation or through teleconnection (e.g., Lu, 2001; Lu and Dong, 2001, Gong and Ho 2002; Zhou et al., 2009, among many others). The diabatic heating due to anomalous SSTs and precipitation is of primary importance in modulating EASM system, particularly the WNPSH (Rodwell and Hoskins, 2001; Liu et al., 2004). To make a clear picture of AO-related heating, here we investigated the tropical atmospheric heat budget in spring and summer with respect to MAM AO extremes. We analyzed the apparent heating rate (Q1) and moisture sinks (Q2) which are defined as the residual terms of the thermodynamic equation (Yanai et al. 1973; Ding 1989), and expressed as the followings;

$$Q1 = c_p \left[\frac{\partial T}{\partial t} + V \cdot \nabla T + \left(\frac{p}{p_0} \right)^{R_d/c_p} \omega \frac{\partial \theta}{\partial p} \right]$$

$$Q2 = -L \left(\frac{\partial q}{\partial t} + V \cdot \nabla q + \omega \frac{\partial q}{\partial p} \right);$$

where the constants of c_p , R_d , and L are respectively the specific heat for dry air, gas constant for dry air, and the latent heat of deposition. T is the temperature, P and P_0 are pressures at a specific level and the reference level respectively, V the horizontal wind, θ the potential temperature, ω the vertical p -velocity, and q the specific humidity. The Q1 and Q2 are calculated for all levels from surface to 200 hPa using NCEP-NCAR reanalysis daily data. The apparent heating rate of large-scale motion system consists of the heating due to radiation, the release of latent heat by net condensation, and vertical convergence of the vertical eddy transport of sensible heat. And the apparent moisture sink consists of the net condensation and vertical divergence of the vertical eddy transport of moisture. Therefore, the vertical integration of Q1–Q2 measures the sensible and latent heat fluxes from the surface to the atmosphere. The positive values indicate net heat gains of the atmosphere and negative values indicate net heat loss. In the present study, we analyzed the integrated Q1–Q2 from surface to 200 hPa, and their seasonal mean values were obtained by averaging all daily data for each year. We employed a composite analysis of heating anomalies corresponding to AO extremes to highlight the possible AO

signals. To avoid the possible influence of inter-decadal climate variations and possible data discontinuity, we confined the reference period to 1979–2008, a period of better data quality in the NCEP-NCAR reanalysis dataset. ENSO dominates the tropical precipitation and temperature, which should be taken into account when performing the composite analysis. After excluding large Niño3 SST years when the mean SST anomalies from the previous December to May exceeds $\pm 0.5^\circ\text{C}$, we selected the highest five MAM AO years from 1979 to 2008, namely 1990, 2007, 2003, 2002, and 1982. These years are marked by ‘Q’ in Fig. 6. The spring and summer means for these 5 years are calculated, and their anomalies are obtained after subtracting their respective climate means.

Figure 7 displays the composites of vertical integrations of Q1–Q2 for spring and summer. It is clear that the tropospheric atmosphere gains anomalous heats with a positive anomaly center along the equator between 150°E – 170°W , where the heat budget changes from $+15$ to $+45 \text{ W m}^{-2}$. The positive anomalies spread northwards to about 30°N in 160°E . This is consistent with the results of regression analysis by Nakamura et al. (2007). Using reanalysis II data from 1979–2004, they found that corresponding to one unit standard deviation of spring MAM AO index the atmosphere between 150°E – 180° gains the sensible and latent heat by $+5$ to $+10 \text{ W m}^{-2}$ as integrated from 1,000 to 200 hPa. In JJA, the anomalous heating center appears in the similar region with maximum of $+15$ – $+30 \text{ W m}^{-2}$ heating rate. Figure 7 clearly shows that the major features in summer and spring bear much similarity, except that the significant area in summer becomes smaller than spring and the center shifts to the west by about 10 degrees. In association with the anomalous heating, we would expect evident upward air motions.

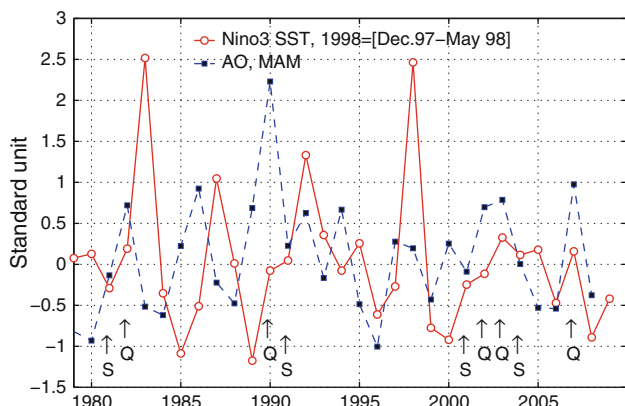


Fig. 6 Spring AO and winter-spring Niño 3 SST. ‘Q’: indicating years used for making composites of heating anomalies (including 1982, 1990, 2002, 2003 and 2007). ‘S’: indicating years of AO-forcing simulation experiments (including 1981, 1991, 2001 and 2004)

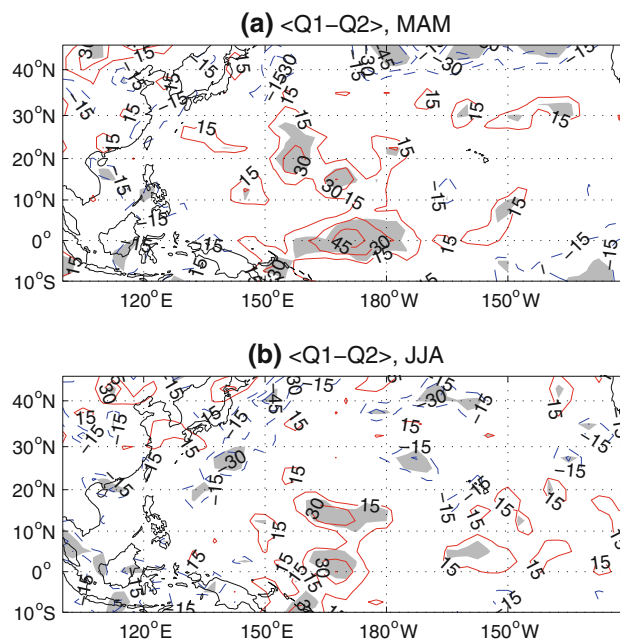


Fig. 7 Distribution of the anomalous heats in MAM and JJA. Shown as the means of 1982, 1990, 2002, 2003 and 2007 minus the means of 1979–2008. The heats are measured as the vertically integrated Q1–Q2 from surface to 200 hPa. Units: W m^{-2} . The significant (at the 90% level) regions are shaded

Plotted in Fig. 8 are the zonal and vertical winds in the pressure–longitude section along 10°N which is selected according to the maxima of AO–SST correlations (Fig. 4). During spring the anomalous ascending air motion appears in 140°E – 170°E and the significant winds span from the surface up to 150 hPa level. The maxima of ascending steadily keep the location thereafter, centering around 135°E – 170°E in summer. The anomalous upward air motion would result from the heating. The upward winds would bring more precipitation which, in turn, helps maintain the anomalous ascending by latent heats. Note the positive precipitation anomalies of $+1$ to $+2 \text{ mm/day}$ consistently appear in around the anomalous SSTs (see Figs. 4, 5). In general, the distribution of SSTs, heating and precipitation anomalies agrees well with each other in physical meanings. The observed features of the anomalous heating over tropics support the fact that MAM AO is significantly related to the anomalous equatorial SSTs and air–sea interaction. The persistent heating through JJA also implies that the air–sea interaction would serve as sustaining forcing to reinforce/feedback to the spring AO-related cyclonic atmospheric circulation over the western North Pacific.

It should be pointed out that climate anomalies in association with AO phases may be asymmetrical. For example, Sung et al. (2010) indicated the asymmetrical downstream consequences of NAO in boreal winter. Comparing the positive- and negative-AO composites of

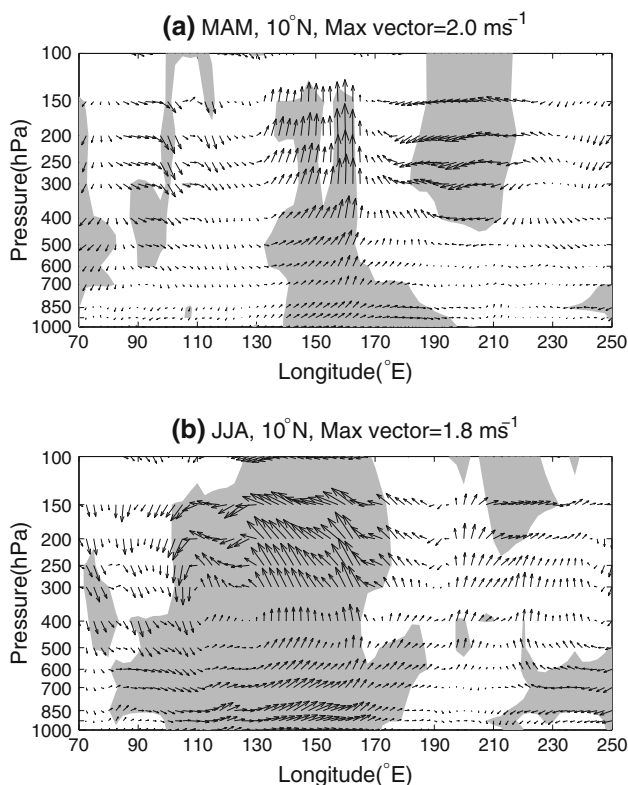


Fig. 8 Pressure-longitude section along 10°N, showing MAM and JJA wind anomalies of u, w in association with one-unit-larger MAM AO index. For clarity the w has been multiplied by 1,000. Units: ms^{-1} . Shadings indicate values significant at the 95% level

heating could help to clarify this problem after excluding the influence of other factors (such as ENSO, continental snow cover, and so on). As can be found in Fig. 6, however, when the ENSO years are excluded we could hardly find enough negative AO events comparable to its positive counterpart. The same problem remains when making composites for circulation, SSTs, and precipitation. The long-term simulation data could help clarify/test this question.

4.3 Atmospheric dipole in the North Pacific

AO simply describes the strength of the westerly winds in high latitudes. During positive AO years, the westerly significantly weakens over Asia–Pacific sector. In particular, the jet stream and storm track activity weaken together (Limpasuvan and Hartmann 1999; Ambaum et al. 2001; Chang and Fu 2002). The interaction between synoptic transient disturbances and the jet stream is an important internal source of the monthly mean circulation anomalies, which might be related to the appearance of the atmospheric dipole over the North Pacific in association with AO. Theoretically, the transient eddy-induced mean circulation changes due to barotropic processes could be

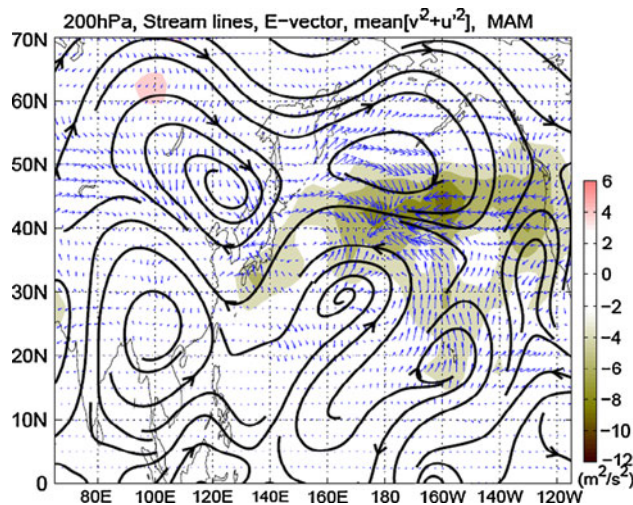


Fig. 9 Changes of E-vectors ($\overline{v'^2 - u'^2}, -\overline{u'v'}$), eddy kinetic energy (shadings) and seasonal mean circulation streamlines (smooth lines with arrows) in March–April–May at 200 hPa. All are shown as anomalies in association with a one-unit-larger MAM AO index. Maximum E-vector anomaly is $+10.1 \text{ m}^2\text{s}^{-2}$

given by the divergence of Eliassen-Palm vector. A local region vectors convergence will be characterized by the forcing of anticyclonic vorticity to the north of the convergence region and cyclonic vorticity forcing to the south. The net effect is that convergence is associated with easterly acceleration of the mean flow and divergence with westerly acceleration (James 1994). For the sake of simplicity, we computed the anomalies of the 200 hPa level extended Eliassen-Palm flux (E-vector), which is defined as $(\overline{v'^2 - u'^2}, -\overline{u'v'})$ (James 1994). Here u and v are the zonal and meridional wind components, respectively. The overbars represent time averages from March 1 through May 31. The primes denote departures from the mean. The v' and u' are computed from the Butterworth band-pass filter retaining components with time periodicity of 1–6 days. As shown in Fig. 9, the E-vector convergence is predominant over the region of 160°E–170°W, 35°N–45°N. To the north of the convergence core an anomalous anticyclone in MAM mean flow at 200 hPa level appears in 160°E–150°W, 40°N–65°N. Immediately, a cyclonic anomaly is located to the south side, spanning from about 20°N–40°N, 140°E–170°E. This dipole structure of the seasonal mean flow anomaly agrees quite well with the theoretical analysis. In addition, the eddy kinetic energy ($\overline{v'^2 + u'^2}$) evidently weakens in the north Pacific with negative extrema in about 170°E–150°W. The AO-related zonally elongated pattern shown in Fig. 9 is very similar to the third EOF of the 500 hPa storm tracks in north Pacific in Lau (1988, figure 2c). Lau (1988) computed the composites of monthly mean 300 hPa heights in association with EOF3,

and found that the negative extrema (i.e., below-normal synoptic-scale activity) are accompanied by an anticyclone in north 40°N and a cyclone in the south. This dipole pattern resembles the eddy-induced height tendency composite taking the vorticity transport of transient eddies into account (Lau 1988, figures 11e and 11f), where the effect of the eddy heat transport is considerably weak (Lau and Holopainen 1984). Agreement of our results with theoretical and observation analyses strongly suggests that the interaction between mean-flow and synoptic-scale eddy probably plays an important role in generating the MAM mean circulation anomalies in association with AO. It should be pointed out that the possible roles of AO-related boundary forcings (such as land/ocean thermal anomalies) in influencing the monthly mean atmospheric circulation in MAM and the AO-EASM relations have to be studied further.

4.4 A hypothetical explanation

In previous sections, we show the significant SST changes in association with spring AO over the North Pacific, including the warming in the tropics and the extra-tropics, and the cooling between them. Note that the extra-tropical anomalies in atmosphere and SST weaken gradually after MAM, and almost disappear in JJA. In contrast, the tropical anomalies persist from spring through summer. The maintaining of anomalous cyclonic circulation in the tropical western North Pacific seemed to be essential in linking spring AO to summer East Asian climates. Because atmospheric circulation itself has a short memory, the maintenance of the anomalous cyclonic circulation from MAM to JJA should rely on the tropical SSTs. Here we suppose a hypothetical explanation that the air-sea interaction in the tropical western North Pacific plays a key role in sustaining the spring AO-related circulation through summer.

During positive AO springs, there is a tripole pattern of SSTs over the North Pacific which is tightly related to the basin scale atmospheric dipole (i.e., an anomalous cyclone in the tropical western Pacific and an anticyclone in the extratropics). More important is the consequent tropical SST anomalies where above-normal atmosphere heat budget exists. In the presence of the mean easterly winds in tropics, the anomalous cyclonic circulation reduces the total wind speed in 150°E – 180° , and the weaker evaporation, weaker vertical water mixing, and weaker upwelling induce warmer SST anomalies. Previous studies revealed that the tropical heating, mainly concentrated to the north of the equator, shortly produces an anomalous cyclone to the northwestern side of the heat source as a stationary Rossby response of the atmosphere (Matsuno 1966; Gill 1980). Through this well-known Gill-type mechanism, the

SST anomaly in turn enhances the cyclone and the westerlies in the tropical western Pacific. This positive feedback would sustain from spring to summer. As the anomalous cyclone extends to 105°E in JJA, positive vorticity anomalies appear in South China and the South China Sea. The weakened western North Pacific subtropical high would reduce the moisture transporting from the south oceans, and also causes a lower pressure gradient to its northwest side and thus a weaker Mei-yu front (Chang et al. 2001; Gong and Ho 2002). As a result, a drier climate in Meiyu-Changma-Baiu belt and a wetter climate to the south are observed in June–July–August. It is noteworthy that Wang et al. (2000) and Wang and Zhang (2002) reported a similar positive feedback mechanism for connecting Niño SST and EASM, and emphasized the importance of the Philippine Sea anomalous anticyclone, which appears to the west of the anomalous cyclone. In our analysis, however, the cyclone emerges without its counterpart of anticyclone to the west. Differences might be due to their heating locations. Niño SST heating is located in the central to east tropics, about 30 degrees east of the AO-related heating. The former straddles in equator but the later locates slightly north to the equator. This mechanism of AO-EASM connection is further tested later by numerical experiments.

5 Simulations of AO-related SSTs and atmospheric circulation

5.1 Background and numerical models

Observations show that there are large-scale anomalous SSTs in the North Pacific, particularly the warmer-than-normal SSTs in the tropics persist multi-months. In spring, the SST signals are strong, which is hypothesized to trigger the air-sea interactions and to maintain anomalous cyclonic circulations till summer. Numerous studies have proven that the tropical SSTs are an important forcing of mid-high latitude atmospheric circulations. For example, Quadrelli and Wallace (2002) indicated that the AO circulation might depend on ENSO phases. During warmer tropic SST years, the Arctic center of AO is more prominent. At the same time, the reversed sea level pressure anomalies out of the Arctic center develop much broader and encompass the entire tropics. In upper levels, an equatorward displacement of the jet stream and the storm tracks are observed. In addition to the AO, the tropical SSTs can also generate/modulate the variability of atmospheric teleconnections such as the Pacific-North America pattern (e.g., Trenberth et al. 1998; among others). In this study, we found that the SST anomalies in the North Pacific are remarkable in association with AO and AO-related atmospheric

circulation. Thus an arisen question is whether the anomalous atmospheric circulation in spring is a response to, rather than a forcing of, the North Pacific SSTs (particularly the tropical SSTs). In this section we address this problem in two steps. First, in order to examine whether the AO-related circulation can generate the observed SSTs (particularly the tropical warming), we performed numerical simulations using an ocean model. Second, to identify the AO-related consequences of atmospheric circulation from MAM through JJA in conjunction of the air-sea interaction, we performed simulations with prescribed spring AO-related wind stresses using an atmosphere-ocean coupled climate model.

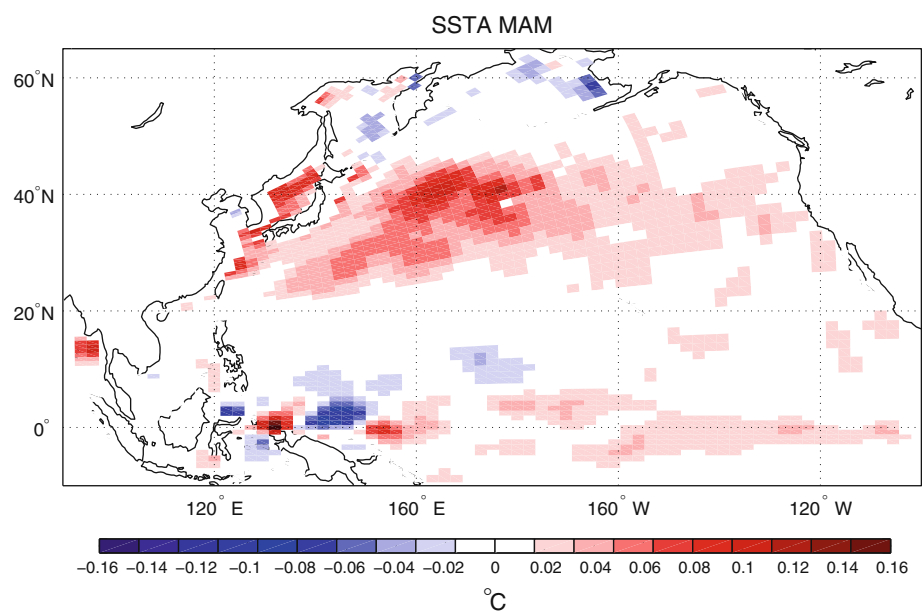
The model used in the present study is the Bergen Climate Model version 2 (BCM2). The atmosphere component of BCM2 consists of the spectral atmospheric general model ARPEGE/IFS (Déqué et al. 1994). In this study, the ARPEGE has a horizontal resolution of approximately 2.8° and 30 levels in the vertical. The ocean component of BCM2 is the Miami Isopycnic Coordinate Ocean Model (MICOM) (Bleck et al. 1992). The horizontal resolution is 2.4° along the equator with one pole over Siberia and the other over the South Pole. The meridional spacing near equator is 0.8° to better resolve equatorial-confined dynamics. The MICOM has 34 isopycnic layers in the vertical and a non-isopycnic surface mixed layer on top providing the linkage between the atmospheric forcing and the ocean interior. Details of the BCM2 can be found in Furevik et al. (2003) and Otterå et al. (2009). The stable climates for present-day conditions are achieved by running BCM2 for 600 years, on which the below numerical experiments are based.

5.2 Atmosphere forced SSTs

In this atmosphere forced experiment, we performed one control run and four sensitivity runs. For the control run the MICOM is forced by the NCEP-NCAR reanalysis atmospheric circulation from January 1, 1948 to December 31, 2007. The four sensitivity simulations have been carried out for 1981, 1991, 2001, and 2004, respectively. These 4 years are chosen because in these years both spring AO and winter-spring Niño3 SSTs are nearly normal (see Fig. 6). Each of the four runs starts from January 1 and ends on December 31, i.e., simulating one whole year. Different from the control run, in sensitivity runs the anomalous surface wind fluxes have been imposed on the NCEP-NCAR fluxes during spring (i.e., from March 1 to May 31). The 850 hPa wind anomalies corresponding to one-unit stronger MAM AO are used as the AO-forcing of atmosphere. In our simulation the anomalous AO-forcing is confined within the domain 120°E – 120°W , 0° – 65°N (see Fig. 4a). To enhance the AO-related atmosphere signals, the imposed surface wind fluxes have been multiplied by 2-times of standard deviation. The average SSTs of four sensitivity simulations minus the control run for the same 4 years represent the anomalous SSTs responding to the AO-forcing of atmosphere.

Figure 10 displays the spatial distribution of the SST anomalies. A dominant feature is the large-scale warming over the extratropics, with a maximum center spanning along 40°N and extending southwestward to the east of Japan. South of 20°N , the slight surface cooling appears. It is noteworthy that the evident warming found in the observation along the equator is well reproduced, spanning

Fig. 10 Simulated SST anomalies in spring, shown as the AO-wind forcing experiments minus the control runs. Simulated years are 1981, 1991, 2001 and 2004



from 140°E eastward to about 110°W. The maximum SST centers appear between 140°E and 180°, slightly to north of the equator. Generally, the SST response to AO-related circulation agrees well with the observed SST anomalies in spring (Fig. 4). The results from numerical simulations suggest the AO-related atmospheric circulation anomalies triggered the basin-scale SST change, particularly the warming anomaly in the central Pacific along the equator. A slightly different feature from the observations is the cooling in south of 20°N, that is much weaker than observation. The difference may be because our experiments considered only atmospheric forcing on ocean. After taking into account the positive feedback of air-sea interaction, the location and magnitude of tropical SSTs appeared to be more realistic as demonstrated in the next section using atmosphere–ocean coupling simulations. It is interesting to note that the central tropical Pacific tends to be warmer in high MAM AO years, suggesting a sign of El Niño. Previous studies suggested that the spring AO could trigger ENSO events (Nakamura et al. 2006, 2007). However, it is still unclear whether/how a central-Pacific or an eastern-Pacific ENSO is developed (Ashok et al. 2007; Ashok and Yamagata 2009; Kao and Yu 2009). There is a possibility that AO may influence EASM through ENSO. This interesting issue is still an open question. Overall, the AO-related warmer tropical SSTs are keys to understanding AO-EASM links.

5.3 Coupled simulations of the atmospheric circulation

Using BCM2 atmosphere–ocean coupling model, we performed a control run and one sensitivity run. The control run was integrated for 10 years, starting from January 1. During this simulation the atmosphere and ocean freely interact. The same initial conditions are employed in the sensitivity run. Different from the control run, the observed AO-related wind stresses are repeatedly imposed on the North Pacific Ocean. They are the same domain and wind stresses as used as in the previous ocean simulation. The AO-related wind stresses are purposely imposed on the North Pacific from March 1 through April 30, leaving May as a ‘buffer’ window to reduce the possible influence of the abrupt removal of the imposed forcing. The simulated JJA 850 hPa winds are averaged from the 10-year control run and from sensitivity integrations, respectively. Theoretically, the difference of the means is caused by the MAM AO-related atmospheric forcing.

Figure 11 displays the distribution of the 850 hPa wind difference in JJA (the sensitivity minus the control runs). The observed tropical atmosphere circulation features in association with MAM AO are generally well reproduced in the coupled simulations. An anomalous cyclone over the northwestern Pacific is evident, with the center locating

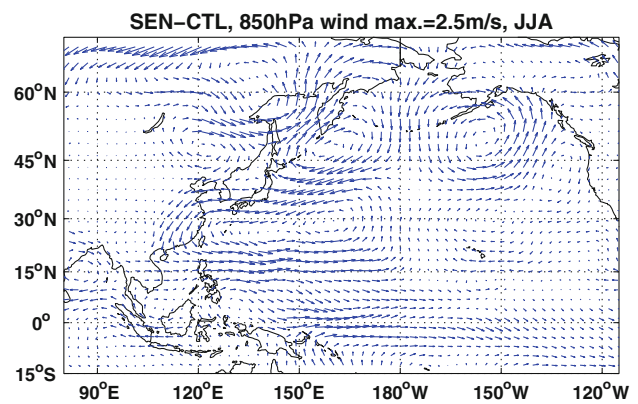


Fig. 11 Simulated 850 hPa wind anomalies. The 10-year sensitive integration minus the 10-year control runs

over 100°E–180° south of 35°N. Note that the observed westerly winds dominate over 120°E–180° in south of 15°N (Fig. 4d), while the simulated westerly winds appear between equator and about 20°N, extending about 5 degrees northward. This seemed to be mainly caused by the similar northward shift of the anomalous cyclone. Given the fact that in our sensitivity simulations, we did not consider any high-latitude process (such as the Arctic sea ice/SST, land surface conditions over Eurasia, and North Atlantic SSTs), the high similarity between the simulated tropical winds and the observations in JJA manifest the importance of North Pacific air-sea interaction in producing the anomalous circulation through JJA when responds to MAM AO.

We also examined the simulated SSTs. The positive SST anomalies in the central equatorial Pacific persists from MAM through JJA. The center of SSTs covers a region from about 140°E to 140°W, and slightly spans eastward from MAM to JJA. The positive anomalies over the eastern North Pacific and the cooling in mid-latitude over the western North Pacific are also comparable with the observation (c.f. Figures 4 and 11), although their locations are about 5 degrees farther to the north than the observation. These spatial distribution of the simulated SSTs are consistent with the simulated atmospheric circulations, which generally agree with the observation. It is worthy to note that the simulated circulations north of 40°N show some structured signals. We speculate that this might arise from the lack of mid-high latitude processes. If both tropical and high-latitude AO-related forcings (within/beyond the North Pacific) are included, the circulation anomalies in high latitudes could be more similar to the observation. On the other hand, the simulated anomalous cyclone in the western North Pacific appears as the most outstanding feature. This implies that the role of air-sea interaction over the North Pacific (particularly in the central-western tropics) dominate other mechanisms (such as

the influence from mid-high latitudes). This mechanism is also supported by the numerical simulation of BCM2 atmosphere model, which is forced by prescribed SSTs. The SSTs are prescribed as the MAM-AO related positive anomalies over 5°S–15°N, 140°E–160°W with a warm center at 160°E and 5°N, while outside this region, the SSTs are prescribed as climatology. The sensitivity experiment minus the control run yields an anomalous cyclone in south of 20°N, 120°E–180°, and this suggests that the AO-related SSTs in the western tropical Pacific forces the atmosphere and produces/reinforce the cyclone (figure not shown). Overall, the circulation anomalies in the sensitivity simulations indicate that a positive EASM monsoon condition is produced in summer in response to positive AO-related atmosphere circulation anomalies in spring.

6 Discussion

We note that the year-to-year variations of MAM AO and EASM virtually match each other better since the late 1970s (Fig. 1a), whereas, prior to this time their agreement seems poor. This unsteady relationship is also apparent in the WNPSH time-series (Fig. 3b). Thus an arisen question is whether the MAM AO-EASM relationship was shifted with time. To investigate this further, we examined correlations between MAM AO and Wang and Fan (1999) index, the WNPSH, and the mean JJA precipitation for 10 stations along the Meiyu belt. A better agreement of these indices with spring AO after 1979 is quite obvious. As listed in Table 2, the correlation between EASM index and MAM AO changes from 0.07 for 1951–1978 to a significant value of 0.47 after 1979. For the WNPSH, the correlations change from 0.03 to –0.48 and for the Meiyu precipitation, they change from –0.17 to –0.46.

In the present study, we have suggested a mechanism of the air-sea interaction over the North Pacific in connecting spring AO and EASM climates. If this mechanism is true, why did it work better since the late 1970s than prior to that

time? To find a clue for this problem, we examined the SSTs and atmospheric circulation for the two sub-periods of 1951–1978 and 1979–2008. Figure 12 demonstrates that the warmer SSTs in the central Pacific appear in MAM and persist through JJA in both time periods. The anomalous atmospheric cyclones are also located in the western North Pacific. The western branch of the anomalous cyclone is located farther away from the Asian continent during the early period, while it moves to the west closer to the continent in the latter period. This difference in the location of the western margin of the cyclones between the two periods seems to be the partial cause for the different EASM response to spring AO-related atmosphere. We hypothesize that the EASM system transition which occurred in the late 1970s might play roles in the AO-monsoon relationship shift. Climate shift around 1979 over East Asia is manifest in monsoon precipitation and atmospheric circulation. An outstanding feature in middle troposphere is the westward extension of the WNPSH after the late 1970s (Gong and Ho 2002; Zhou et al. 2009). As well-known, the East Asian climates are sensitive to the location of the subtropical high. The AO-related anomalous cyclone may exert different influence on East Asian climates depending on the background state of the WNPSH (particularly its location). The western flank of the WNPSH is located far away from the Asian continents in around 130°–140°E during 1958–1979 in NCEP/NCAR and ERA40 data sets. During 1980–1999 its location moves westward to around 120°E (see figure 1 in Zhou et al. 2009). The subtropical high sitting closer to East Asia during 1979–2008 seemed to lead to more sensitive monsoon climate responses when modulated by the AO-related cyclone. Observation and modeling studies suggested that the Indian Ocean and western Pacific SSTs are (at least partly) responsible for the decadal shift of the WNPSH (Gong and Ho 2002; Zhou et al. 2009). How the AO-EASM relationship are influenced/modulated by the decadal shift of East Asian climate system, what are the roles of SSTs in the Indian Ocean, the tropical Pacific or the North Atlantic (Gu et al. 2009), whether this shift of AO-EASM relationship are related to the strengthening ENSO-EASM relationship since the late 1970s (Wang et al. 2008b), however, are all uncertain at the moment and these require a substantial investigation and a physical testing.

Table 2 Correlations between MAM AO and EASM variables for two time periods. Based on interannual time-scale components and ENSO signals removed

	Before 1979	After 1979
Wang and Fan (1999) index, JJA	+0.07	+0.47 ^a
Western North Pacific Subtropical High, JJA	+0.03	–0.48 ^a
Mean Meiyu precipitation of 10 stations, JJA	–0.17	–0.46 ^b

^a Significant at the 95% level

^b Significant at the 90% level

7 Conclusion

As a conclusion, in the present study the significant spring AO-EASM relationship is supported by the consistent changes in EASM indices, the summer precipitation and the three-dimensional atmospheric circulation over East Asia and the western North Pacific. Following a positive

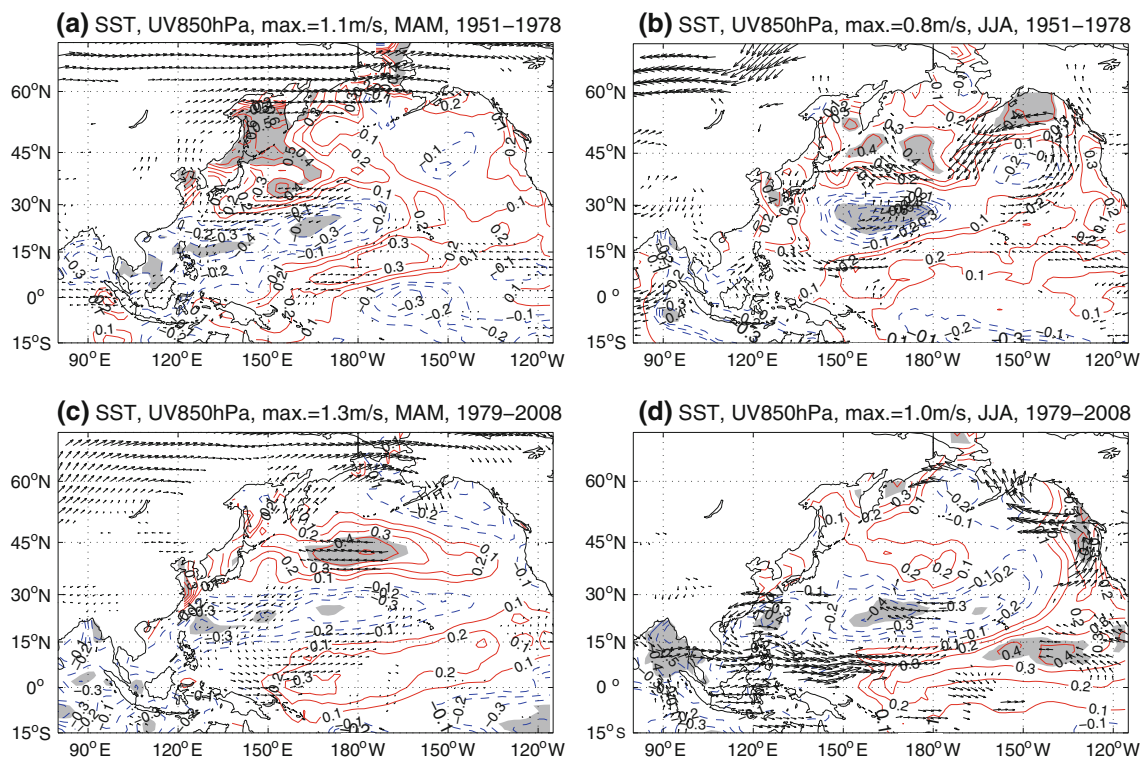


Fig. 12 Observed spring AO-related SST and 850 hPa circulations in MAM and JJA for two periods of 1951–1978 and 1979–2008. Contour lines are correlation coefficients between AO and SST (solid lines: positive correlations, and dashed the negative, shadings:

significant at the 95% level). The vectors are significant (95% level) anomalies of 850 hPa wind corresponding to one-unit-larger MAM AO index. For interannual time scale and ENSO signals removed

spring AO, three monsoon indices tend to be stronger in summer. Meanwhile, there appears an anomalous cyclonic circulation at 850 hPa in southeastern Asia and western Pacific in summer, implying an enhanced monsoon trough activity in lower troposphere. At the same time the summer western North Pacific subtropical high gets weaker, yielding a smaller pressure gradient to the northwestern side of the high and weaker northward moisture transporting. Consistently, the positive precipitation anomalies are located over a broad region south of 30°N stretching from southern China to the western Pacific and negative anomalies appear in the lower valley of the Yangtze River and southern Japan.

The possible linking mechanism of the spring AO-summer monsoon connections is investigated with focus on the atmospheric and oceanic changes over the North Pacific. In association with spring positive AO, the tropospheric circulation over the North Pacific displays a dipole structure with an anomalous cyclone located over the tropics between 120°E–160°W and an anticyclone located over the extra tropics. Associated with the atmospheric circulation, there are well-defined patterns in SST, whose positive anomalies appear in the central to eastern Pacific south of 15°N and negative anomalies around 150°E–

180°E and 15°N–30°N. The ocean model simulations suggest that the spring SSTs are triggered by the AO-atmosphere circulations. The AO-induced tropical cyclonic circulation and positive SSTs near the equator persist their locations and strength until summer, playing key roles in connecting spring AO to EASM by a positive air-sea feedback. The warmer SSTs near the equator produced by the cyclone result in anomalous diabatic heating. The sensible and latent heating, in turn, intensifies the cyclone through a Gill-type response of the atmosphere. The atmosphere–ocean coupled climate model captures the cyclonic anomalies, and this feature is also found in an atmosphere simulation forced by MAM-AO related SSTs over the central tropical Pacific. Through this positive feedback the tropical atmosphere and SST patterns are maintained from spring to summer and consequently modify the monsoon trough and the western North Pacific subtropical high. This eventually leads to a drier climate in regions of Meiyu-Changma-Baiu belt and a wetter climate to the south in June–July–August. This mechanism linking spring AO-EASM, to authors' knowledge, has not been clearly addressed in previous studies, and provides new information to better understand/predict the East Asian summer monsoon.

Acknowledgments This work was supported by the PE10030 and PE10130 and in part by PE11010s of Korea Polar Research Institute. DY Gong was supported by 2008AA121704, 2007BAC29B02, and GYHY200706010. The numerical experiments and part of analysis has been supported by the Norwegian Research Council through the East Asian DecCen (no 193690) project. Reanalysis data were obtained from <ftp://www.ftp.cdc.noaa.gov>. The comments and suggestions of two anonymous reviewers are appreciated.

References

- Adler RF, Huffman GJ, Chang A, Ferraro R, Xie P, Janowiak J, Rudolf B, Schneider U, Curtis S, Bolvin D, Gruber A, Susskind J, Arkin P (2003) The version 2 global precipitation climatology project (GPCP) monthly precipitation analysis (1979-present). *J Hydrometeorol* 4:1147–1167
- Ambaum MHP, Hoskins BJ, Stephenson DB (2001) Arctic Oscillation or north Atlantic Oscillation? *J Clim* 14:3495–3507
- Ashok K, Yamagata T (2009) The El Niño with a difference. *Nature* 461:481–484
- Ashok K, Behera SK, Rao SA, Weng H, Yamagata T (2007) El Niño Modoki and its teleconnection. *J Geophys Res* 112(C11007). doi:10.1029/2006JC003798
- Bamzai AS (2003) Relationship between snow cover variability and Arctic Oscillation on a hierarchy of time scales. *Int J Climatol* 23:131–142. doi:10.1002/joc.854
- Bleck R, Rooth C, Hu D, Smith LT (1992) Salinity-driven thermocline transients in a wind-and thermohaline-forced isopycnic coordinate model of the North Atlantic. *J Phys Oceanogr* 22:1486–1505
- Branstator G (2002) Circumglobal teleconnections, the jetstream waveguide, and the North Atlantic Oscillation. *J Clim* 15:1893–1910
- Buermann W, Lintner B, Bonfils C (2005) A wintertime Arctic Oscillation signature on early-season Indian Ocean monsoon intensity. *J Clim* 18:2247–2269
- Chang KM, Fu YF (2002) Interdecadal variations in northern hemisphere winter storm track intensity. *J Clim* 15:642–658
- Chang C-P, Zhang Y, Li T (2000a) Interannual and interdecadal variations of the East Asian summer monsoon and tropical Pacific SSTs. Part 1: role of the subtropical ridge. *J Clim* 13:4310–4325
- Chang C-P, Zhang Y, Li T (2000b) Interannual and interdecadal variations of the East Asian summer monsoon and tropical Pacific SSTs. Part 2: Southeast China rainfall and meridional structure. *J Clim* 13:4326–4340
- Chang C-P, Harr P, Hu JH (2001) Possible roles of Atlantic circulations on the weakening Indian monsoon rainfall-ENSO relationship. *J Clim* 14:2376–2380
- Déqué M, Drevetton C, Braun A, Cariolle D (1994) The ARPEGE/IFS atmosphere model: a contribution to the French community climate modeling. *Climate Dynamics* 10:249–266
- Ding YH (1989) Diagnosis methods in dynamic meteorology. Science Press, pp 293, (in Chinese)
- Feng S, Hu Q (2008) How the North Atlantic multidecadal oscillation may have influenced the Indian summer monsoon during the past two millennia. *Geophys Res Lett* 35:L01707. doi:10.1029/2007GL032484
- Folland CK, Knight J, Linderholm HW, Fereday D, Ineson S, Hurrell JW (2009) The summer North Atlantic Oscillation: past, present, and future. *J Clim* 22:1082–1103
- Fu CB, Zeng ZM (2005) Correlations between North Atlantic Oscillation Index in winter and eastern China Flood/Drought Index in summer in the last 530 years. *Chin Sci Bull* 50(21):2505–2516
- Furevik T, Bentsen M, Drange H, Kindem I, Kvamstø NG, Sorteberg A (2003) Description and validation of the Bergen Climate Model: ARPEGE coupled with MICOM. *Climate Dynamics* 21:27–51
- Gill AE (1980) Some simple solution for heat-induced tropical circulation. *Q J R Meteorol Soc* 106:447–462
- Gong D-Y, Ho C-H (2002) Shift in the summer rainfall over Yangtze River valley in the late 1970s. *Geophys Res Lett* 29(10). doi:10.1029/2001GL014523
- Gong D-Y, Ho C-H (2003) Arctic Oscillation signals in East Asian summer monsoon. *J Geophys Res* 108(D2):4066. doi:10.1029/2002JD002193
- Gong D-Y, Kim S-J, Ho C-H (2009) Arctic and Antarctic Oscillation signatures in tropical coral proxies over the South China Sea. *Ann Geophys* 27:1979–1988
- Goswami BN, Madhusoodanan MS, Neema CP, Sengupta D (2006) A physical mechanism for North Atlantic SST influence on the Indian summer monsoon. *Geophys Res Lett* 33:L02706. doi:10.1029/2005GL024803
- Gu W, Li C, Li W, Zhou W, Chan JCL (2009) Interdecadal unstationary relationship between NAO and east China's summer precipitation patterns. *Geophys Res Lett* 36:L13702. doi:10.1029/2009GL038843
- Hori ME, Yasunari T (2003) NAO impact towards the springtime snow disappearance in the western Eurasian continent. *Geophys Res Lett* 30(19):1977. doi:10.1029/2003GL018103
- James IN (1994) Introduction to circulating atmospheres. Cambridge University Press, Cambridge, p 422
- Kalnay E, Kanamitsu M, Kistler R, Collins W, Deaven D, Gandin L, Iredell M, Saha S, White G, Woollen J, Zhu Y, Chelliah M, Ebisuzaki W, Higgins W, Janowiak J, Mo KC, Ropelewski C, Wang J, Leetmaa A, Reynolds R, Jenne R, Joseph D (1996) The NCEP/NCAR 40-year reanalysis project. *Bull Am Meteorol Soc* 77:431–437
- Kao HY, Yu JY (2009) Contrasting eastern-Pacific and central-Pacific types of ENSO. *J Clim* 22:615–632
- Lau N-C (1988) Variability of the observed midlatitude storm tracks in relation to low-frequency changes in the circulation pattern. *J Atmosph Sci* 45(19):2718–2743
- Lau N-C, Holopainen EO (1984) Transient eddy forcing of the time-mean flow as identified by geopotential tendencies. *J Atmosph Sci* 41(3):313–328
- Lau K-M, Kim K-M, Yang S (2000) Dynamical and boundary forcing characteristics of regional components of the Asian summer monsoon. *J Clim* 13(14):2461–2482
- Li J, Yu RC, Zhou TJ, Wang B (2005) Why is there an early spring cooling shift downstream of the Tibetan Plateau. *J Clim* 18(22):4660–4668
- Limpasuvan V, Hartmann DL (1999) Eddies and the annular modes of climate variability. *Geophys Res Lett* 26(20):3133–3136
- Liu YM, Wu GX, Ren RC (2004) Relation between the subtropical anticyclone and diabatic heating. *J Clim* 17:682–698
- Lu R (2001) Interannual variability of the summertime North Pacific subtropical high and its relation to atmospheric convection over warm pool. *J Meteorol Soc Jpn* 79:771–783
- Lu R, Dong BW (2001) Westward extension of North Pacific subtropical high in summer. *J Meteorol Soc Jpn* 79:1229–1241
- Lu R, Dong B, Ding H (2006) Impact of the Atlantic Multidecadal Oscillation on the Asian summer monsoon. *Geophys Res Lett* 33:L24701. doi:10.1029/2006GL027655
- Matsuno T (1966) Quasi-geostrophic motions in the equatorial area. *J Meteorol Soc Jpn* 44:25–42

- Miller AJ, Zhou S, Yang SK (2003) Relationship of the Arctic and Antarctic Oscillations to the outgoing longwave radiation. *J Clim* 16:1583–1592
- Nakamura T, Tachibana Y, Honda M, Yamane S (2006) Influence of the northern hemisphere annular mode on ENSO by modulating westerly wind bursts. *Geophys Res Lett* 33:L07709. doi:10.1029/2005GL025432
- Nakamura T, Tachibana Y, Shimoda H (2007) Importance of cold and dry surges in substantiating the NAM and ENSO relationship. *Geophys Res Lett* 34:L22703. doi:10.1029/2007GL031220
- Ogi M, Tachibana Y, Yamazaki K (2004) The connectivity of the winter North Atlantic Oscillation (NAO) and the summer Okhotsk High. *J Meteorol Soc Jpn* 82(3):905–913
- Otterå OH, Bentsen M, Bethke I, Kvamstø NG (2009) Simulated pre-industrial climate in Bergen Climate Model (version 2): model description and large-scale circulation features. *Geosci Model Develop* 2:197–212
- Quadrelli R, Wallace JM (2002) Dependence of the structure of the Northern Hemisphere annular modes on the polarity of ENSO. *Geophys Res Lett* 29(23):2132. doi:10.1029/2002GL015807
- Rodwell MJ, Hoskins BJ (2001) Subtropical anticyclones and summer monsoons. *J Clim* 14:3192–3211
- Smith TM, Reynolds RW, Peterson TC, Lawrimore J (2008) Improvements to NOAA's historical merged land-ocean surface temperature analysis (1880–2006). *J Clim* 21:2283–2293
- Sui C-H, Chung P-H, Li T (2007) Interannual and interdecadal variability of the summertime western North Pacific subtropical high. *Geophys Res Lett* 34:L11701. doi:10.1029/2006GL029204
- Sung MK, Kwon W-T, Baek H-J, Boo K-O, Lim G-H, Kug J-S (2006) A possible impact of the North Atlantic Oscillation on the east Asian summer monsoon precipitation. *Geophys Res Lett* 33:L21713
- Sung M-K, Lim G-H, Kug J-S (2010) Phase asymmetric downstream development of the North Atlantic Oscillation and its impact on the East Asian winter monsoon. *J Geophys Res* 115:D09105. doi:10.1029/2009JD013153
- Tao SY, Chen LX (1987) A review of recent research on the East Asian summer monsoon in China. In: Chang C-P, Krishnamurti TN (eds) *Monsoon meteorology*. Oxford University Press, Oxford, pp 60–92
- Thompson DWJ, Lorenz DJ (2004) The signature of the annular modes in the tropical troposphere. *J Clim* 17:4330–4342
- Thompson DWJ, Wallace JM (1998) The Arctic Oscillation signature in the wintertime geopotential height and temperature fields. *Geophys Res Lett* 25:1297–1300
- Trenberth KE, Branstator GW, Karoly D, Kumar A, Lau NC, Ropelewski C (1998) Progress during TOGA in understanding and modeling global teleconnections association with tropical sea surface temperatures. *J Geophys Res* 103:14291–14324
- Wang B, Fan Z (1999) Choice of South Asian summer monsoon indices. *Bull Am Meteorol Soc* 80:629–638
- Wang B, Zhang Q (2002) Pacific-East Asian teleconnection. Part II: how the Philippine Sea anomalous anticyclone is established during El Niño development. *J Clim* 15:3252–3264
- Wang B, Wu R, Fu X (2000) Pacific-East Asian teleconnection: how does ENSO affect East Asian climate? *J Clim* 13:1517–1536
- Wang B, Wu Z, Li J, Liu J, Chang C-P, Ding Y, Wu G (2008a) How to measure the strength of the East Asian summer monsoon? *J Clim* 21:4449–4464
- Wang B, Yang J, Zhou T, Wang B (2008b) Interdecadal changes in the major modes of Asian–Australian monsoon variability: strengthening relationship with ENSO since the late 1970s. *J Clim* 21:1771–1789
- Wang Y, Li S, Luo D (2009) Seasonal response of Asian monsoonal climate to the Atlantic Multidecadal Oscillation. *J Geophys Res* 114:D02112. doi:10.1029/2008JD010929
- Watanabe M (2004) Asian jet waveguide and a downstream extension of the North Atlantic Oscillation. *J Clim* 17:4674–4691
- Wu Z, Wang B, Li J, Jin F-F (2009a) An empirical seasonal prediction model of the East Asian summer monsoon using ENSO and NAO. *J Geophys Res* 114:D18120. doi:10.1029/2009JD011733
- Wu BY, Yang K, Zhang RH (2009b) Eurasian snow cover variability and its association with summer rainfall in China. *Advances Atmos Sci* 26(1):31–44. doi:10.1007/s00376-009-0031-2
- Yang S, Lau K-M, Kim K-M (2002) Variations of the east Asian jet stream and Asian-Pacific-American winter climate anomalies. *J Clim* 15:306–325
- Yanai M, Esbensen S, Chu J-H (1973) Determination of bulk properties of tropical cloud clusters from large-scale heat and moisture budgets. *J Atmos Sci* 30:611–627
- Yu R, Zhou TJ (2004) Impacts of winter-NAO on March cooling trends over subtropical Eurasia continent in the recent half century. *Geophys Res Lett* 31(12):L12204. doi:10.1029/2004GL019814
- Zhang QY, Tao SY, Chen LT (2003) The interannual variability of East Asian summer monsoon indices and its association with the pattern of generation circulation over East Asia. *Acta Meteorologica Sinica* 61:559–568 (in Chinese with English Abstract)
- Zhou TJ, Yu R, Zhang J, Drange H, Cassou C, Deser C, Hodson DLR, Sanchez-Gomez E, Li J, Keenlyside N, Xin X, Okumura Y (2009) Why the western Pacific subtropical high has extended westward since the late 1970s. *J Clim* 22:2199–2215